Aust. J. Phys., 1979, **32**, 231–54

An Investigation of the Accuracy of Numerical Solutions of Boltzmann's Equation for Electron Swarms in Gases with Large Inelastic Cross Sections

Ivan D. Reid

Electron and Ion Diffusion Unit, Research School of Physical Sciences,
Australian National University; present address: Mawson Institute for Antarctic Research,
University of Adelaide, G.P.O. Box 498, Adelaide, S.A. 5001.

Abstract

A Monte Carlo simulation technique has been used to test the accuracy of electron energy distribution functions and transport coefficients calculated using conventional numerical solutions of Boltzmann's equation based on a two-term approximation. The tests have been applied to a number of model gases, some of which have characteristics close to those of real gases, and include cases where the scattering is anisotropic. The results show that, in general, previous application of the numerical solution to real gases has been valid.

1. Introduction

The acquisition of an increasingly large body of experimental cross section data for low energy electron–atom and electron–molecule collisions from both beam and swarm experiments has enabled a number of intercomparisons to be made between the data from the different experimental approaches, often with somewhat disappointing results (see e.g. Schulz 1976; Land 1978). Where there is most overlap between the data from the two kinds of experiment, that is, in the range from about 0·5 to 20 or 30 eV, the cross section data from swarm experiments are derived from an analysis of transport measurements made at values of E/N (ratio of electric field strength to gas number density) where there is an increasing possibility that the transport theory customarily used in the analysis (see e.g. Huxley and Crompton 1974) is no longer sufficiently accurate. The purpose of the present paper is to examine quantitatively the conditions that are likely to lead to a breakdown of the theory in situations where the energy transfer is dominated by inelastic scattering and E/N is large. The work extends earlier studies of a similar kind that were limited to transport in atomic gases where it was assumed that the scattering was entirely elastic (e.g. Milloy and Watts 1977; Braglia 1977).

Considerable attention has been focused recently on attempts to extend the range of validity of transport theory for weakly ionized gases. A recent review by Skullerud (1977) summarizes the work up to 1977. Some of this work has indicated in a general way the conditions under which solutions of Boltzmann's equation based on a two-term spherical harmonics expansion of the velocity distribution function (together with other approximations consistent with such an approximation) are likely to fail (see e.g. Ferrari 1977), but quantitative estimates of the extent of the failure, in terms of the magnitude of the errors in calculated distribution functions and transport coefficients, have not been given.

The application of Monte Carlo techniques to the determination of collision cross sections from measured electron transport coefficients has been reported in several recent papers; for example, by Hunter (1977) and Blevin *et al.* (1978) who analysed data for H_2 for values of E/N up to 200 Td (1 Td $\equiv 10^{-17}$ V cm^2), and Saelee and Lucas (1977) whose work applied to H_2 and CO in the range of E/N from 30 to 3000 Td. However, there has been as yet no comparison between these results and those obtained from a Boltzmann analysis applied to the same set of cross sections.

In order to examine quantitatively the validity of the conventional Boltzmann transport theory as applied to molecular gases (Holstein 1946; Frost and Phelps 1962; Gibson 1970), Monte Carlo simulations have been used in this paper to determine the transport properties of electron swarms in model gases with various combinations of elastic and inelastic cross sections, and in some cases with anisotropic scattering. The results so obtained are compared with those from a standard numerical solution of the Boltzmann equation to highlight the combination of circumstances that leads to significant errors in the results from the conventional analysis, and to indicate the magnitude of these errors.

A brief resume of the assumptions that underlie the first-order solution of the Boltzmann equation is given in Section 2. The Monte Carlo simulation techniques used in the present work are described in Section 3, and the various models and results obtained with them are described in Section 4. The significance of the results and their implications for the analysis of the transport data for some real gases are discussed in Section 5.

2. Solutions of Boltzmann's Equation

The usual way of relating the spatial and temporal variation of an electron swarm to the collision processes that determine the swarm characteristics is through a solution of the Boltzmann equation. This equation relates the rate of change of the population of an element of six-dimensional phase space due to the presence of an electric field and electron density gradients to that resulting from collisions with the gas molecules, and its solution provides the spatial and velocity distribution functions for the electrons in the swarm in terms of the cross sections for the elastic and inelastic collision processes.

A solution of the equation that takes full account of the boundary conditions in a specific experimental situation is difficult to achieve, and several approaches have been adopted to reduce the problem to a tractable form (see e.g. Huxley and Crompton 1974 and references therein). The simplest approach, and the one most widely used to determine collision cross sections from the data from swarm experiments, is based on the assumption that the transport coefficients inferred from the motion of the swarm are independent of both the initial form of the distribution function $F(\boldsymbol{r}, \boldsymbol{v})$ and the presence of the boundaries. The effect of the latter can be minimized by choosing experimental conditions that ensure that the influence of the boundaries is confined to a region that is a small fraction of the total critical dimension of the apparatus (for example, in a mobility experiment, the drift distance). With this assumption, which requires justification in each instance, the electron motion can be characterized by a spatially invariant velocity distribution function $f(\boldsymbol{v})$ which can be computed by solving the Boltzmann equation incorporating an assumed set of cross sections. From $f(\boldsymbol{v})$ the transport coefficients can be calculated for comparison with corresponding experimental data.

Even with the simplifying assumption just described the equation cannot be readily solved, and further assumptions have been made to facilitate a solution. This paper is concerned with the errors in the transport coefficients arising from the latter assumptions, which are briefly outlined below.

We first define, for a process with the differential scattering cross section $\sigma_\Omega(\gamma, g)$, the following integral cross sections:

$$\sigma_0(g) = 2\pi \int_0^\pi \sigma_\Omega(\gamma, g) \sin\gamma \, d\gamma,$$

$$\sigma_1(g) = 2\pi \int_0^\pi \sigma_\Omega(\gamma, g) \cos\gamma \sin\gamma \, d\gamma,$$

$$\sigma_m(g) = \sigma_0(g) - (g'/g)\sigma_1(g),$$

where γ is the scattering angle and g and g' are the relative speeds before and after a collision between an electron and a gas molecule. Since we have the electron–neutral mass ratio $m/M \ll 1$, it is usually assumed that negligible error is made by replacing γ by θ and g and g' by v and v' respectively where θ, v and v' are the quantities measured in the laboratory frame which correspond to γ, g and g'. This assumption has been adopted throughout the present work. The above equations define the total cross section σ_0 and the momentum transfer cross section σ_m. Note that when the collision is elastic we have $v'/v \approx g'/g = 1$ and the momentum transfer cross section for elastic collisions is

$$\sigma_{m,e}(v) = \sigma_{0,e}(v) - \sigma_{1,e}(v).$$

For a gas with inelastic channels with threshold energies $\varepsilon_k = \frac{1}{2}mv_k^2$, there are corresponding excitation and de-excitation cross sections denoted by $\sigma_{0,k}$ and $\sigma_{1,k}$, and $\sigma_{0,-k}$ and $\sigma_{1,-k}$ respectively.

The electron velocity distribution function $f(\boldsymbol{v})$ under consideration is that which applies to both a spatially uniform distribution of electrons or to the whole of an isolated electron swarm. In the absence of an electric field, $f(\boldsymbol{v})$ is spherically symmetrical, but the application of a field $\boldsymbol{E}$ results in a distorted distribution which maintains symmetry about the field direction and can be conveniently represented by an expansion in Legendre polynomials:

$$f(\boldsymbol{v}) = f_0(v) + \sum_{l=1}^{\infty} f_l(v) \, P_l(\cos\phi),$$

where ϕ is the angle between $\boldsymbol{v}$ and $\boldsymbol{E}$.

As a simplifying assumption, which is valid when the departure from spherical symmetry is small (low field case), it has usually been assumed that the expansion can be truncated after the second term without introducing serious error, in which case

$$f(\boldsymbol{v}) = f_0(v) + f_1(v)\cos\phi. \tag{1}$$

Substitution of equation (1) into the time and spatially independent form of Boltzmann's equation then leads to an equation that can be separated into two

equations, one representing conservation of population and the other the conservation of momentum for electrons within a given speed (energy) range. The speed range v to $v+\mathrm{d}v$ can be represented by the volume element in velocity space bounded by spherical surfaces of radii v and $v+\mathrm{d}v$ (see e.g. Huxley and Crompton 1974). The conservation of population is then equivalent to the invariance of the number of representative points marking the ends of the vectors $\boldsymbol{v}$ in this volume element (spherical shell), and the equation describing this conservation is

$$\frac{\mathrm{d}}{\mathrm{d}v}\left(\tfrac{1}{3}v^2 a f_1(v) - \chi_{\mathrm{coll}}(v)\right) = 0, \tag{2}$$

where $a = eE/m$, and $4\pi\chi_{\mathrm{coll}}(v)$ represents the net flux of points across the spherical surface of radius v due to collisions.

When only elastic collisions occur, the equation describing the conservation of momentum is

$$a\,\mathrm{d}f_0/\mathrm{d}v = -N\sigma_{\mathrm{m,e}}(v)\,v f_1(v). \tag{3}$$

The equation is more complex when both elastic and inelastic collision processes occur. If we disregard for the moment the effect of superelastic (de-excitation) collisions then equation (3), modified to include inelastic collisions, becomes

$$a\frac{\mathrm{d}f_0}{\mathrm{d}v} = -\left\{N\sigma_{\mathrm{m,e}}(v) + \sum_k \left(N\sigma_{0,k}(v)\,v - \{N\sigma_{1,k}(v_{1,k})\,v_{1,k}\}\frac{v_{1,k}}{v}\frac{f_1(v_{1,k})}{f_1(v)}\right)\right\} f_1(v),$$

where $v_{1,k}^2 = v^2 + v_k^2$. This equation can be formally expressed in the form of equation (3) provided $\sigma_{\mathrm{m,e}}(v)$ is replaced by an equivalent momentum transfer cross section $\sigma_{\mathrm{m}}(v)$ given by

$$\sigma_{\mathrm{m}}(v) = \sigma_{\mathrm{m,e}}(v) + \sum_k \left\{\sigma_{0,k}(v) - \sigma_{1,k}(v_{1,k})\left(\frac{v_{1,k}}{v}\right)^2 \frac{f_1(v_{1,k})}{f_1(v)}\right\}.$$

Terms similar to the second and third terms are added when account is taken of superelastic collisions.

Because of the much greater energy exchange in an inelastic collision compared with an elastic collision, the presence of an inelastic collision process can drastically modify the energy distribution function even in situations where the cross section for that process is very much smaller than the elastic cross section. Consequently in many cases where inelastic collisions play an important role the second and third terms in the expression for $\sigma_{\mathrm{m}}(v)$ are small compared with the first. In any case, the third term vanishes when inelastic scattering is isotropic. Thus it is often justified to omit the third term (and a corresponding term for superelastic collisions) and adopt the approximation

$$\sigma_{\mathrm{m}}(v) = \sigma_{\mathrm{m,e}}(v) + \sum_k \{\sigma_{0,k}(v) + \sigma_{0,-k}(v)\}. \tag{4}$$

From the pair of equations (2) and (3) (with $\sigma_{\mathrm{m,e}}(v)$ replaced by $\sigma_{\mathrm{m}}(v)$ when inelastic scattering occurs) a single equation in $f_0(v)$ can be obtained. By integrating the equation once and expressing it in terms of the electron energy $\varepsilon = \frac{1}{2}mv^2$, we obtain

the following equation when there is both elastic and inelastic scattering (Holstein 1946; Frost and Phelps 1962):

$$\left(\frac{(eE)^2\varepsilon}{N\sigma_m(\varepsilon)}+(6m/M)\kappa T\varepsilon^2 N\sigma_{m,e}(\varepsilon)\right)\frac{df_0(\varepsilon)}{d\varepsilon}$$
$$+(6m/M)\varepsilon^2 N\sigma_{m,e}(\varepsilon)f_0(\varepsilon)+3N\sum_k J_k(\varepsilon)=0, \tag{5a}$$

where

$$J_k(\varepsilon)=\int_\varepsilon^{\varepsilon+\varepsilon_k}\{f_0(y)-f_0(y-\varepsilon_k)\exp(-\varepsilon_k/\kappa T)\}\sigma_{0,k}(y)\,y\,dy,$$

with κ being the Boltzmann constant and T the gas temperature. The normalizing relation for $f_0(\varepsilon)$ is

$$\int_0^\infty \varepsilon^{\frac{1}{2}} f_0(\varepsilon)\,d\varepsilon=1.$$

The second and third terms of equation (5a) which account for the energy exchange in elastic collisions are small compared with the other terms when the cross sections for inelastic scattering are comparable with the elastic scattering cross section, and they can become comparable only when the inelastic cross sections are very small compared with the elastic cross section. Thus, in most circumstances, negligible error results from the replacement of $\sigma_{m,e}(\varepsilon)$ by $\sigma_m(\varepsilon)$ in these terms. It is thus usual (e.g. Frost and Phelps 1962) to write equation (5a) as

$$\left(\frac{(eE)^2\varepsilon}{N\sigma_m(\varepsilon)}+(6m/M)\kappa T\varepsilon^2 N\sigma_m(\varepsilon)\right)\frac{df(\varepsilon)}{d\varepsilon}$$
$$+(6m/M)\varepsilon^2 N\sigma_m(\varepsilon)f(\varepsilon)+3N\sum_k J_k(\varepsilon)=0, \tag{5b}$$

where here, and in what follows, $f_0(\varepsilon)$ has been replaced by $f(\varepsilon)$ for convenience of notation.

While the replacement of $\sigma_{m,e}$ by σ_m in equation (5a) may be valid, in the same circumstances the reverse substitution of $\sigma_{m,e}$ for σ_m may lead to large errors. Thus it is important to note that, if equation (5b) is used to determine $f(\varepsilon)$, the momentum transfer cross section that appears in the equation is the *total* cross section for momentum transfer (as given by equation 4) and not the cross section for momentum transfer in elastic collisions.

Equation (5a) or (5b) may be solved numerically and the drift velocity v_{dr} and lateral diffusion coefficient $D_\perp$ calculated from the relations (see e.g. Huxley and Crompton 1974)

$$v_{dr}=-\frac{eE}{3N}\left(\frac{2}{m}\right)^{\frac{1}{2}}\int_0^\infty \frac{\varepsilon}{\sigma_m(\varepsilon)}\frac{df}{d\varepsilon}\,d\varepsilon, \tag{6}$$

$$ND_\perp=\frac{1}{3}\left(\frac{2}{m}\right)^{\frac{1}{2}}\int_0^\infty \frac{\varepsilon}{\sigma_m(\varepsilon)}f(\varepsilon)\,d\varepsilon. \tag{7}$$

Solutions of equation (5b) have been given, for example, by Frost and Phelps (1962) and by Gibson (1970). The solution and code developed by Gibson were used in the present investigation.

Equations (5b), (6) and (7) are developed on the assumptions implicit in equation (1) and matching approximations in the Boltzmann collision terms (see e.g. Ferrari 1977), together with the approximation used to obtain equation (4). Since the purpose of the present work is to compare results obtained from the above analysis with those determined from a Monte Carlo simulation, where accuracy is only limited by statistical uncertainty, it is not essential to model real gases. Relatively simple models could therefore be chosen (see Section 4 below) in which elastic scattering was accompanied by a single inelastic process having a threshold energy and energy loss ε_i. The gas temperature was taken to be zero, thus avoiding the need to account for either the thermal motion of the gas molecules or superelastic collisions in the simulations.

3. Monte Carlo Simulations

(a) *Monte Carlo methods for determining electron trajectories*

Two methods were used in the present study: a 'direct' method, suitable for simulating electron motion when the cross section has a simple dependence on the electron speed; and the faster and more versatile 'null collision' method, which was developed in the latter stages of the comparison.

Direct Method

This method was used for most of the simulations, and is essentially that used by McIntosh (1974) but modified to include the effects of inelastic collisions. The method of determining the electron trajectories by the use of random numbers is as follows.

Let P be the probability that the time of free flight of an electron is less than or equal to some value T. Then, if n_0 electrons commence paths with similar trajectories, $n_0 P$ electrons collide before time T while $n = n_0(1-P)$ continue on the original trajectory after time T. If $\nu(v) = N\sigma_0(v)v$ is the collision frequency then, of n electrons, the number $\mathrm{d}n$ making a collision within a time interval $\mathrm{d}t$ is $n\nu(t)\,\mathrm{d}t$. Thus

$$\mathrm{d}n = -n\nu(t)\,\mathrm{d}t,$$

and it follows that, of an initial number n_0, the number that have not collided at time T is found from

$$\ln(n/n_0) = -\int_0^T \nu(t)\,\mathrm{d}t = -N\int_0^T \sigma_0(v)\,v(t)\,\mathrm{d}t.$$

Thus

$$n = n_0 \exp\{-N\,X(T)\},$$

where

$$X(T) = \int_0^T \sigma_0(v)\,v(t)\,\mathrm{d}t, \tag{8}$$

and it follows from the definition of P that

$$P = 1-\exp\{-NX(T)\} \quad \text{or} \quad X(T) = -N^{-1}\ln(1-P). \tag{9a, b}$$

It can be shown (see e.g. Hammersley and Handscomb 1964) that if R is a random number uniformly distributed in the interval [0, 1] then R is related to some probability density $p(x)$ by

$$R = \int_0^y p(x)\,\mathrm{d}x,$$

where y is a random variable drawn from the distribution $p(x)$. In the present case, the distribution is the distribution of free times. It follows that the distribution of free times T and free paths $S(T)$ can be found by choosing a random number R and solving equation (9b) with P replaced by R.

In the simulations, the electric field $\boldsymbol{E}$ is aligned in the $-z$ direction so that the acceleration of the electrons $\boldsymbol{a} = -e\boldsymbol{E}/m$ is in the $+z$ direction. If $\boldsymbol{v}(t)$ is the velocity of an electron at time t after the last collision, with components $v_x(t) = v_x$, $v_y(t) = v_y$ and $v_z(t) = v_z(0)+at$, then we have

$$v(t) = \{v^2(0) + 2at\,v_z(0) + a^2t^2\}^{\frac{1}{2}}. \tag{10}$$

While $X(T)$ is simply related to P, the free time T cannot be found readily from equation (8) unless the right-hand side of the equation is integrable. Milloy and Watts (1977) performed the integration using the trapezoidal rule, terminating the summation at the value of $t = T$ when the equation was satisfied. In the present work, advantage was taken of the fact that the integration can be performed for certain energy dependences of the cross section. For example, if the cross section is constant, that is, $\sigma_0(v) = \sigma$, then

$$X(T) = \sigma S(T) = \tfrac{1}{2}\sigma a^{-1}\{v_z(T)\,v(T) - v_z(0)\,v(0) + v_\rho^2(\operatorname{arsinh}\{v_z(T)/v_\rho\} - \operatorname{arsinh}\{v_z(0)/v_\rho\})\}, \tag{11}$$

where $v_\rho^2 = v_x^2+v_y^2 = v^2(t)-v_z^2(t)$. On the other hand, if the cross section is linearly dependent on energy, that is, $\sigma_0(v) = kv^2$, then

$$X(T) = \tfrac{1}{4}k\{a^{-1}(v_z(T)\,v^3(T) - v_z(0)\,v^3(0)) + 3v_\rho^2\,S(T)\}. \tag{12}$$

With $X(T)$ found from equation (9b) for a given R, equation (11) or (12) was solved for T by making an initial estimate T' of T and using Newton's method to adjust T' until $X(T')$ was within one part in 10^5 of $X(T)$. Usually very few iterations were required to satisfy this condition.

Equation (9b) in conjunction with equation (11) or (12) relates the free time T to the probability P that the free time is less than or equal to T on the assumption that the simple energy dependence of the cross section upon which either (11) or (12) is based remains unchanged over the entire length of the free path. However, some modification to the method of relating T to P is required whenever the electron crosses the inelastic threshold either through gaining energy by travelling in the direction of the electric force or losing energy by travelling against it.* In this event

* Throughout this paper simple models are considered in which there is a single inelastic process with a threshold energy $\varepsilon_k \equiv \varepsilon_i$. In what follows therefore the arguments apply to this situation only, although they can be extended without difficulty to the case of a number of inelastic processes. To simplify the terminology from here on the subscript 0 is omitted from the symbol denoting total cross sections. Thus the total elastic cross section $\sigma_{0,e}$ is denoted by σ_e and the total inelastic cross section $\sigma_{0\,i}$ by σ_i.

the electron enters an energy regime where the equation for $X(t)$ used up to that time no longer applies, since the energy dependence of the cross section assumes a different form. The modification consists of treating the free path remaining after the electron crosses the threshold as if it were a new free path, determining the probability P_B that a collision will occur at or before a time T_B after the threshold has been crossed, and relating the residual free time T_B to P_B using a form of equation (11) or (12) appropriate to the situation that exists after the threshold has been crossed.

Having selected a random number R, we must first determine whether R is greater than P_A, the probability that a collision will occur before the electron reaches the threshold energy. If we find $R > P_A$ then P_B can be calculated from R and P_A since the total probability of collision P ($\equiv R$) is the sum of P_A and the product of P_B and the probability of the electron not having collided before traversing the threshold energy. Thus

$$R = P_A + (1-P_A)P_B \qquad \text{or} \qquad P_B = (R-P_A)/(1-P_A).$$

Once P_B has been determined, $X(T_B)$ and hence T_B can be found. The collision point that terminates the free path can thus be determined, the position of the electron having been updated at the time of crossing the threshold.

When the energy of the electron at the point of collision is above the threshold energy a further random number R' is generated to determine the collision type. If we have

$$R' \leqslant \sigma_e(u)/\{\sigma_e(u)+\sigma_i(u)\},$$

where u is the speed at the time of collision, then the collision is considered to be elastic. Otherwise it is taken to be inelastic.

Null Collision Method

A major drawback to the direct method is the fact that only certain functional dependences of $\sigma(v)$ can be easily treated. However, it is ultimately desirable to be able to model particular cases where the Boltzmann analysis is suspect, so a simulation method which can use arbitrary cross sections is required. A method which has this property is the null collision method proposed by Skullerud (1968) and recently used by Lin and Bardsley (1977) to model ion swarms.

For a given set of elastic and inelastic cross sections a null collision cross section $\sigma_n(v)$ is defined so that

$$\sigma(v) = \sigma_e(v) + \sum_k \sigma_k(v) + \sigma_n(v) = Cv^{-1},$$

where C is a constant chosen so that we have $\sigma_n(v) > 0$ over the energy range of interest. In the present work, which is restricted to a single inelastic cross section $\sigma_i(v)$, the equation becomes

$$\sigma(v) = \sigma_e(v) + \sigma_i(v) + \sigma_n(v) = Cv^{-1}.$$

Hence, from the probability P, the time between two collision events is readily calculated since (from equations 8 and 9b)

$$T = -(NC)^{-1}\ln(1-P). \tag{13}$$

Once the time of the collision event is established, so too is the velocity u and position of the electron when the collision event occurs. A new random number R is then generated to determine which type of collision event takes place. If we have

$$\sigma_e(u)/\sigma(u) = u\sigma_e(u)/C > R,$$

then the collision is taken to be elastic; if we have

$$u\sigma_e(u) < CR < u\{\sigma_e(u)+\sigma_i(u)\},$$

then the collision is taken to be inelastic; and if we have

$$u\{\sigma_e(u)+\sigma_i(u)\} < CR,$$

then a null collision is considered to occur. In a null collision there is no change in the velocity of the electron, so that this type of event has no effect on the motion of the electron. Thus the artifice of the null collision cross section has an effect only on the computation of the collision times, which it considerably simplifies. Furthermore, since only the cross sections at the time of a collision event are required, the cross sections may have any functional dependence on v or may be interpolated from a listing of the cross sections.

A null collision simulation, because of its simplicity, takes significantly less computer time than a simulation using the direct method. The efficiency of the program is dependent on the proportion of null collision events, which can be reduced by dividing the energy range into two regions with a different value of C for each region. This minimizes the increase in $\sigma_n(v)$ as v approaches zero in situations where $\sigma_0(v)$ decreases less rapidly than as v^{-1}. If an electron crosses the boundary during its free path, the situation is treated in the same way as it is when an electron crosses the inelastic threshold in the direct method. Using this modification, null collision simulations took only about 50% of the computer time required for a direct simulation. In the several cases where results from the two methods were compared, no significant differences were found.

A further benefit of the null collision method, which was not explored, is that it can be easily used with more than one inelastic cross section.

(*b*) *Kinematics of collisions*

In either simulation method, once the time and type of a real collision have been determined, the position, velocity components, direction cosines c_x, c_y and c_z of the velocity, and energy of the electron at the time of the collision are calculated. It is then necessary to determine the initial direction of the electron after scattering. When the scattering is isotropic, the angles that the direction makes with the three cartesian axes are randomly chosen and their direction cosines c_x', c_y' and c_z' are obtained. The scattering angle θ is then determined from

$$\theta = \arccos(c_x c_x' + c_y c_y' + c_z c_z'). \tag{14}$$

However, when the scattering is anisotropic the following procedure was adopted.

Let $I(\theta)$ be a function that describes the angular dependence of a given scattering process. Then the function

$$\mathscr{I}(\theta) = I(\theta) \Big/ \int_0^{\pi} I(\theta) \sin\theta \, \mathrm{d}\theta \tag{15}$$

is a function such that $\mathscr{I}(\theta)\sin\theta \, \mathrm{d}\theta$ is the probability that an electron will be scattered within $(\theta, \mathrm{d}\theta)$. From the argument given in subsection (*a*) above relating a probability density function (in this instance $\mathscr{I}(\theta)\sin\theta$) to a random number R chosen from the interval [0, 1], it follows that

$$R = \int_0^{\theta'} \mathscr{I}(\theta) \sin\theta \, \mathrm{d}\theta . \tag{16}$$

Thus, for example, if we have $I(\theta) = \sin(\frac{1}{2}\theta)$ then

$$R = \sin^3(\tfrac{1}{2}\theta') \qquad \text{or} \qquad \theta' = 2\arcsin(R^{\frac{1}{3}}) .$$

It is also necessary to determine a random azimuthal angle ϕ for the final velocity vector that represents scattering through an angle θ from the incident direction. This angle is selected from a uniform distribution in the interval $0 \leqslant \phi < 2\pi$. The axis $\phi = 0$ is defined to be one of the normals to the incident direction parallel to the xy plane.

Except in the special case $c_x = c_y = 0$, the direction cosines c_x', c_y' and c_z' of the recoil velocity are found from θ and ϕ and the direction cosines c_x, c_y and c_z of the incident velocity by using the relations

$$c_x' = c_x\cos\theta - (c_y/A)\cos\phi\sin\theta - (c_x c_z/A)\sin\phi\sin\theta , \tag{17a}$$

$$c_y' = c_y\cos\theta + (c_x/A)\cos\phi\sin\theta - (c_y c_z/A)\sin\phi\sin\theta , \tag{17b}$$

$$c_z' = c_z\cos\theta + A\sin\phi\sin\theta , \tag{17c}$$

where $A = (c_x^2 + c_y^2)^{\frac{1}{2}}$. When we have $c_x = c_y = 0$, then

$$c_x' = \cos\phi\sin\theta , \qquad c_y' = \sin\phi\sin\theta , \qquad c_z' = \cos\theta . \tag{18}$$

Because the mass of the electron is very much smaller than that of the molecule, and since the molecule is considered to be at rest, the recoil energy of the electron after an elastic collision is given by

$$\varepsilon_a = \varepsilon_b\{1 - (4mM/(m+M)^2)\sin^2(\tfrac{1}{2}\theta)\} , \tag{19}$$

where ε_b and ε_a are respectively the energies before and after the collision. For inelastic collisions, the effect of momentum transfer in the collisions was approximated by taking the recoil energy to be

$$\varepsilon_a = (\varepsilon_b - \varepsilon_i)\{1 - (4mM/(m+M)^2)\sin^2(\tfrac{1}{2}\theta)\} ,$$

although no significant differences in the results were obtained when the recoil energy was taken as $\varepsilon_a = \varepsilon_b - \varepsilon_i$. This is to be expected since the recoil energy of the molecule is negligible compared with ε_i.

In the simulations, one electron was followed through several million collisions, with energy and position noted at constant time intervals of the order of a few mean free times. In this way, the average energy and energy distribution were obtained.

The transverse diffusion coefficient $D_\perp$ was determined by noting the change in radial position over 1 to 200 sample times using the relation

$$D_\perp = \lim_{\tau \to \infty} \tfrac{1}{4}\tau^{-1}\langle\{x(t+\tau)-x(t)\}^2+\{y(t+\tau)-y(t)\}^2\rangle . \tag{20}$$

In practice, because of statistical scatter in the averages and because the averages approached a limit quite rapidly, the mean of the results for $\tau = 101$ to 200 sample times was taken as the limit. For comparison, $D_\perp$ was also calculated from equation (7) with the energy distribution function $f(\varepsilon)$ determined from the simulation.

The drift velocity was obtained from the ratio of the total displacement to the total drift time represented in the simulation, that is,

$$v_{dr} = z/t . \tag{21}$$

4. Results

Initially several simple isotropic scattering models were used in order to gain some knowledge of how large the ratio σ_i/σ_e has to be before the first-order Boltzmann analysis leads to errors in the calculated transport coefficients of more than 1% or 2%. Retaining the assumption of isotropic scattering, results were then obtained for a model approximating electron transport in CO in the region where the energy loss is predominantly through vibrational excitation. Finally, a hydrogen-like model was constructed to examine the effect of anisotropic elastic and inelastic scattering.

(a) *Isotropic scattering models*

(i) *'Constant' Cross Sections*

For this model the elastic cross section was everywhere independent of energy and the inelastic cross section increased discontinuously to a constant value at the threshold energy. The properties of the model are listed below.

Molecular weight	$M = 4{\cdot}0$ a.m.u.
Elastic cross section	$\sigma_e = \sigma_{m,e} = 6{\cdot}0\,\text{Å}^2 \quad (\equiv 6{\cdot}0\times10^{-20}\,\text{m}^2)$
Inelastic threshold	$\varepsilon_i = 0{\cdot}2$ eV
Inelastic cross section	$\sigma_i(\varepsilon) = 0$ for $\varepsilon < \varepsilon_i$,
	$= Q$ for $\varepsilon \geqslant \varepsilon_i$, with $0 \leqslant Q \leqslant 10\,\text{Å}^2$
Gas temperature	$T = 0$ K
Gas number density	$N = 10^{17}\,\text{cm}^{-3}$

Simulations were carried out at $E/N = 1{\cdot}0$ and $24{\cdot}0$ Td by following the path of a single electron over a total number of free paths C in excess of 10^6. The estimated uncertainty in the transport coefficients calculated using the Boltzmann code is 0·2%; the values of v_{dr} and $\langle\varepsilon\rangle$ determined by the Monte Carlo method are estimated to have an uncertainty of 1% and the value of $D_\perp$ an uncertainty of

Table 1. Comparison of values of v_{dr} and $\langle\varepsilon\rangle$ for 'constant' cross section models

Here, and in the following tables, values obtained from Boltzmann analysis and Monte Carlo simulation are denoted by (B) and (MC) respectively, while $D_\perp$ values obtained from equation (7) with $f(\varepsilon)$ from Monte Carlo simulation are denoted by (H)

E/N (Td)	Q (Å^2)	C (10^6)	v_{dr} values (10^5 cm s^{-1}) v_{dr}(B)	v_{dr}(MC)	$\langle\varepsilon\rangle$ values (eV) $\langle\varepsilon\rangle$(B)	$\langle\varepsilon\rangle$(MC)
			(a) Step-function inelastic cross section			
1·0	0	10·0	5·26	5·28	0·608	0·604
	0·1	10·0	11·71	11·74	0·129	0·127
	1·5	3·4	14·44	14·32	0·0835	0·0824
	3·0	4·3	14·78	14·62	0·0799	0·0794
	6·0	5·0	15·07	14·84	0·0778	0·0780
24·0	0	20·0	25·8	25·9	14·58	14·63
	0·6	4·2	53·7	53·8	3·40	3·36
	3·0	10·0	96·3	94·9	0·602	0·606
	6·0	5·0	109·8	104·6	0·295	0·294
	10·0	3·5	115·9	105·3	0·201	0·194
			(b) Model 2[A]			
24·0	Q^A	5·0	107·4	100·9	0·2648	0·2635

[A] See page 243 of the text.

Table 2. Comparison of values of $D_\perp$ for 'constant' cross section models

E/N (Td)	Q (Å^2)	C (10^6)	$D_\perp$ values (10^5 cm^2 s^{-1}) $D_\perp$(B)	$D_\perp$(MC)	$D_\perp$(H)
			(a) Step-function inelastic cross section		
1·0	6·0	5·0	0·861	0·850	0·863
24·0	0	20·0	11·94	11·94	11·94
	0·6	4·2	5·10	5·0	
	3·0	10·0	1·649	1·40	1·641
	6·0	5·0	1·055	0·70	1·06
	10·0	3·5	0·903	0·45	0·907
			(b) Model 2[A]		
24·0	Q^A	5·0	1·031	0·687	1·044

[A] See page 243 of the text.

2%.* The values obtained for v_{dr} and $\langle\varepsilon\rangle$ (labelled MC) are compared with those obtained from the Boltzmann analysis (labelled B) in Table 1*a*, while values of the transverse diffusion coefficient are compared in Table 2*a*. The values listed under $D_\perp$(H) were obtained by using equation (7) with the energy distribution function $f(\varepsilon)$ obtained from the Monte Carlo simulation.

When σ_i is less than about $0{\cdot}1\,\sigma_e$ (and at $E/N = 1{\cdot}0$ Td for all values of σ_i) the agreement between the values of the transport coefficients obtained with the two

* Subsequent comparison of these results with analytical results (S. L. Lin, personal communication) and independent Monte Carlo simulations (H. R. Skullerud, personal communication) shows deviations in $D_\perp > 2\%$ for some cases tested. These deviations have been traced to computer round-off errors. However, the differences are not sufficiently large to affect any of the conclusions.

methods is good. However, for $E/N = 24{\cdot}0$ Td significant differences occur for the larger values of σ_i, particularly in the values of $D_\perp$. An examination of the energy distribution functions showed a discontinuity at ε_i in the slope of the functions obtained from the Boltzmann code which was not seen in the functions obtained from the simulations. Since there was no evidence of a discontinuity in the distributions calculated for $E/N = 1{\cdot}0$ Td, it seemed likely that the Boltzmann code was inadequate

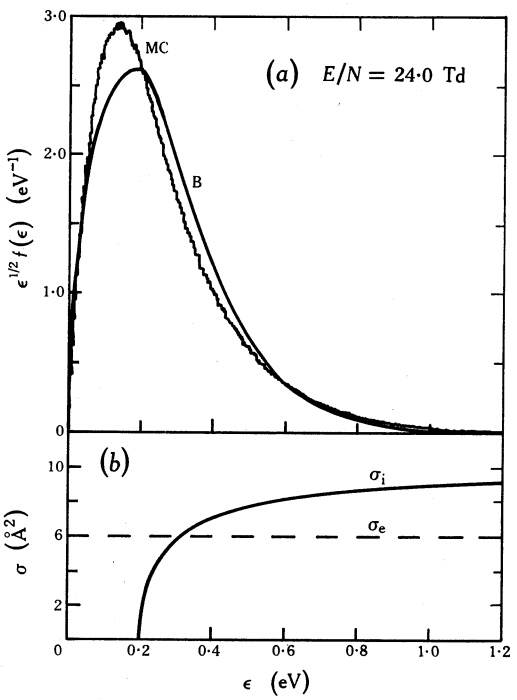

Fig. 1. Plots of (*a*) the electron energy distribution functions $f(\varepsilon)$ obtained from model 2 using two-term Boltzmann analysis (curve B) and Monte Carlo simulation (curve MC). The corresponding elastic and inelastic cross sections are shown in (*b*).

when there were discontinuous changes in the cross sections and a significant proportion of the electron swarm had energies in the vicinity of the discontinuity. To test this hypothesis, comparisons were made using the null collision method and a model (hereafter referred to as model 2) in which the inelastic cross sections did not have a discontinuity at the threshold energy (0·2 eV) but whose magnitude was adjusted to give an energy distribution with a mean energy similar to that for the case of $Q = 6{\cdot}0$ Å^2. The cross section had the analytical form of a rotational excitation cross section corresponding to quadrupole interaction (Gerjuoy and Stein 1955) and was

$$\sigma_i(\varepsilon) = 10{\cdot}0(1 - 0{\cdot}2\varepsilon^{-1})^{\frac{1}{2}} \text{ Å}^2 \qquad (\varepsilon \geqslant 0{\cdot}2). \tag{22}$$

The results of this test are shown in Tables 1*b* and 2*b*; the energy distributions and cross sections are illustrated in Fig. 1. A comparison of the Monte Carlo and Boltzmann transport coefficients for the two models shows similar discrepancies in each case (e.g. $\sim 5\%$ in v_{dr} and $\sim 50\%$ in $D_\perp$), but the distribution function calculated

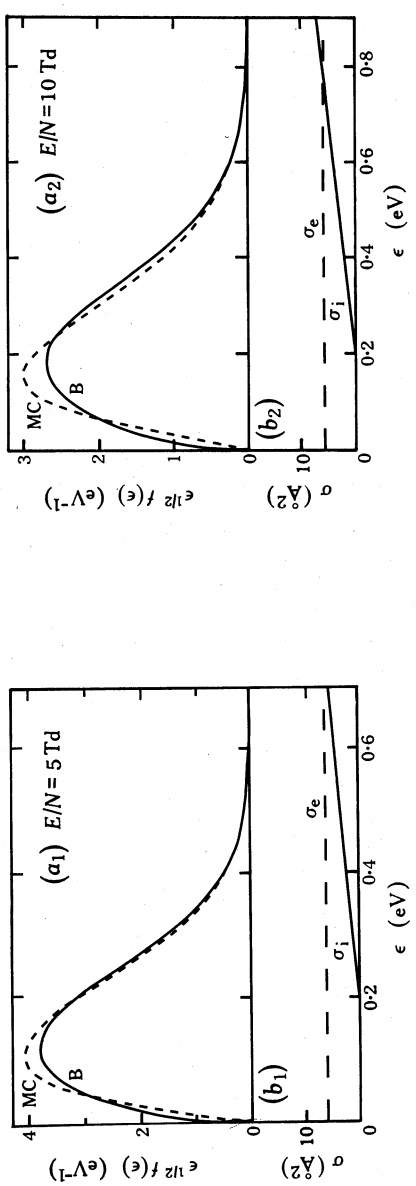

Fig. 2. Representative sample of the energy distribution functions (graphs a_1–a_4) obtained from a 'ramp' inelastic cross section model with $k = 10$ Å^2 eV^{-1} using Boltzmann analysis (B) and Monte Carlo simulation (MC). The corresponding cross sections are shown in each case (b_1–b_4).

from the Boltzmann analysis for model 2 (curve B in Fig. 1*a*) is quite smooth. Thus it seems reasonable to assume that any errors arising from an inability of the Boltzmann code to handle large step-function cross sections are small compared with the errors introduced by the approximations used in its development, and that the overall conclusions that may be drawn from an examination of the data in Tables 1*a* and 2*a* are valid. For this reason the large expenditure of computer time necessary to duplicate the results in these tables using model 2 did not seem justified.

It is interesting to note that:

(1) the errors in the values of v_{dr} calculated using the Boltzmann analysis are much smaller than those in $D_\perp$ in the cases where significant errors arise;

(2) there is generally good agreement between the values of $D_\perp$ derived from equation (7) using the distribution functions obtained by the two methods, even in situations where there are large differences between these values and those derived directly from the simulation using equation (20).

The significance of these trends is discussed in Section 5 below.

(ii) '*Ramp*' *Inelastic Cross Sections*

As a more realistic model than the constant cross section one of the previous section, a model was used that had the same properties as that used in the first set of simulations, except that the inelastic cross section was a linear function of energy; that is,

$$\sigma_i(\varepsilon) = 0 \qquad \text{for} \quad \varepsilon < \varepsilon_i\,, \tag{23a}$$

$$= k(\varepsilon - \varepsilon_i) \quad \text{for} \quad \varepsilon \geqslant \varepsilon_i\,, \qquad \text{with } 0 \leqslant k \leqslant 50\,\text{Å}^2\,\text{eV}^{-1}\,. \tag{23b}$$

A cross section of this form may be used, for example, to approximate the threshold behaviour of some vibrational excitation cross sections.

Several values of k were studied at $E/N = 1{\cdot}0$ and $24{\cdot}0$ Td, while for $k = 10\,\text{Å}^2\,\text{eV}^{-1}$ the investigation was also carried out for a number of values of E/N in the range $1 \leqslant E/N \leqslant 40$ Td. Tables 3 and 4 give the results obtained in these comparisons, while Fig. 2 illustrates some electron energy distributions obtained. The results in Table 3 show trends similar to those which were evident in the constant cross section case. The results in Table 4 show, not unexpectedly, a steadily increasing departure of the results of the Boltzmann analysis from the presumably accurate results of the simulation as E/N increases, due to the steadily increasing ratio of σ_i to σ_e. However, such should not be the case for either of the models discussed in subsection (i) above since, beyond a certain value of E/N, the fraction of the total energy loss accounted for by inelastic collisions (and hence the influence of inelastic collisions on the distribution function) begins to decrease. To demonstrate this, transport coefficients were obtained using model 2 for a range of values of E/N. The comparisons between the Monte Carlo and Boltzmann results are shown in Fig. 3, from which it can be seen that the differences between the results for v_{dr} and $D_\perp$ pass through maximum values at intermediate values of E/N.

(iii) *CO Model*

The ratio of the first vibrational excitation cross section to the elastic scattering cross section is large in CO (Land 1978) and it is therefore possible that conventional

transport theory may be inadequate for analysis of the results of swarm experiments even for relatively small values of E/N. Pointers in this direction are the large normalizing factor that had to be applied by Land to the beam data of Ehrhardt *et al.* (1968) to obtain consistency between these data and the swarm data for v_{dr} and $D_\perp/\mu$, and the inconsistency between the results of Land's analysis of swarm data in pure CO and H. B. Milloy's (personal communication) analysis of v_{dr} data in Ar–CO and He–CO mixtures.

Table 3. Comparison of values of v_{dr}, $\langle\varepsilon\rangle$ and $D_\perp$ for 'ramp' inelastic cross section models

E/N (Td)	k (Å^2 eV^{-1})	C (10^6)	v_{dr} values (10^6 cm s^{-1})		$\langle\varepsilon\rangle$ values (eV)		$D_\perp$ values (10^5 cm^2 s^{-1})		
			v_{dr}(B)	v_{dr}(MC)	$\langle\varepsilon\rangle$(B)	$\langle\varepsilon\rangle$(MC)	$D_\perp$(B)	$D_\perp$(MC)	$D_\perp$(H)
1·0	3·0	5·0	1·177	1·175	0·1187	0·1192	1·071	1·076	1·077
	4·0	5·0	1·202	1·186	0·1139	0·1136	1·050	1·058	1·051
	5·0	5·0	1·221	1·193	0·1105	0·1101	1·034	1·034	1·034
	10·0	5·0	1·275	1·255	0·1016	0·1013	0·990	0·986	0·991
	50·0	5·0	1·379	1·369	0·0882	0·0882	0·921	0·920	0·920
24·0	1·0	5·0	6·87	6·84	1·250	1·251	2·912	2·873	2·921
	2·0	5·0	7·62	7·54	0·885	0·883	2·336	2·221	2·343
	5·0	5·0	8·54	8·39	0·569	0·566	1·754	1·570	1·764
	10·0	5·0	9·15	8·89	0·416	0·413	1·438	1·194	1·452

Table 4. Comparison of values of v_{dr}, $\langle\varepsilon\rangle$ and $D_\perp$ at various E/N for one 'ramp' model

The results shown are for $k = 10$ Å^2 eV^{-1}

E/N (Td)	C (10^6)	v_{dr} values (10^6 cm s^{-1})		$\langle\varepsilon\rangle$ values (eV)		$D_\perp$ values (10^5 cm^2 s^{-1})		
		v_{dr}(B)	v_{dr}(MC)	$\langle\varepsilon\rangle$(B)	$\langle\varepsilon\rangle$(MC)	$D_\perp$(B)	$D_\perp$(MC)	$D_\perp$(H)
1·0	5·0	1·275	1·255	0·1016	0·1013	0·990	0·986	0·991
5·0	5·0	4·36	4·28	0·1742	0·1738	1·226	1·126	1·231
10·0	5·0	6·45	6·27	0·2470	0·2455	1·343	1·175	1·350
15·0	5·0	7·73	7·51	0·312	0·310	1·398	1·189	1·408
20·0	5·0	8·64	8·37	0·371	0·368	1·431	1·197	1·439
24·0	5·0	9·15	8·89	0·416	0·413	1·438	1·194	1·452
30·0	5·0	9·76	9·50	0·480	0·476	1·447	1·196	1·462
40·0	5·0	10·50	10·24	0·579	0·574	1·448	1·188	1·463

As a first step towards a detailed examination of the problem, a model was constructed having a momentum transfer cross section and an effective vibrational excitation cross section that are consistent with electron drift velocities in CO and in He–CO and Ar–CO mixtures (Milloy, personal communication). The molecular weight was taken as 28·01 a.m.u., the inelastic threshold as 0·266 eV, and the gas number density as 10^{17} cm^{-3}. The comparison was made (using the null collision method for the simulation) at $E/N = 20·0$ Td, where a significant fraction of the electron population is above ε_i.

Fig. 4 shows the cross sections for the model and the electron energy distributions obtained by the two methods; the transport coefficients are compared in Table 5*a*. The differences between the transport coefficients are not significant even though there are significant differences in the distribution functions below 0·5 eV. The significance of these results and their extension to include anisotropic inelastic scattering are discussed in Sections 4*b* and 5.

(*b*) *Anisotropic scattering models*

(i) *Isotropic Elastic Scattering, Anisotropic Inelastic Scattering*

As pointed out in Section 2, an assumption usually adopted in the application of equations (5)–(7) is that the inelastic cross section is small compared with the elastic cross section or that the inelastic scattering is reasonably isotropic. It is then justifiable to omit the terms in $v_{1,k}$ from the expression for the effective momentum transfer cross section. The cross section is then given by

$$\sigma_m(v) = \sigma_{m,e}(v) + \sum_k \sigma_{0,k}(v),$$

since there are no superelastic collisions ($T = 0$ K). In the present case we have

$$\sigma_m(v) = \sigma_e(v) + \sigma_i(v). \tag{24}$$

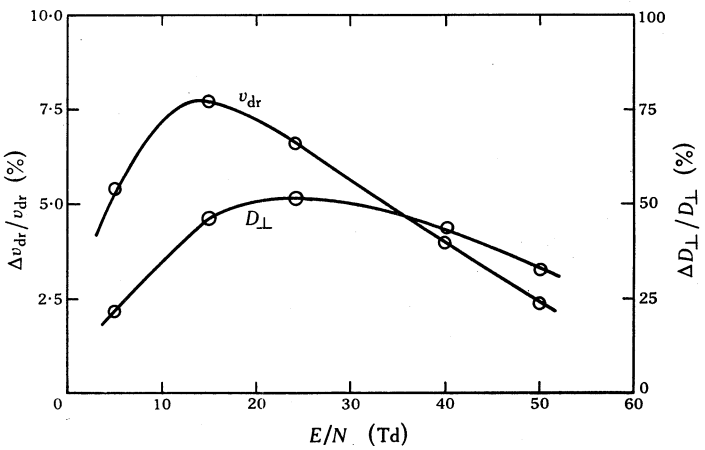

Fig. 3. Discrepancies between the values of v_{dr} and $D_\perp$ calculated using Boltzmann analysis and Monte Carlo simulation with model 2, plotted as a function of E/N.

However, when neither of the conditions above is clearly satisfied the validity of this assumption requires verification. Moreover, the fact that scattering is anisotropic in a proportion of the collisions could lead to a greater anisotropy in the velocity distribution functions and therefore to larger errors from the use of the two-term representations of these functions.

To examine the magnitude of the errors arising from the approximations in the Boltzmann analysis in a situation where only the inelastic scattering was anisotropic, anisotropy in the vibrational excitation collisions was built into the CO model described in subsection *a*(iii) above. In the region of resonant vibrational excitation, the angular scattering distributions are largely independent of energy (Ehrhardt *et al.* 1968) and can be represented to a good approximation by

$$I(\theta) = \tfrac{1}{3} + \tfrac{1}{6}\cos\theta + \tfrac{1}{2}\cos^2\theta.$$

The differential cross section for vibrational excitation $\sigma_{\Omega,i}(v,\theta)$ is given by

$$\sigma_{\Omega,i}(v,\theta) = \tfrac{1}{2}\pi^{-1}\sigma_i(v)\mathscr{I}(\theta), \tag{25}$$

with $\mathscr{I}(\theta)$ related to $I(\theta)$ by equation (15).

Monte Carlo simulations were made using the cross section given by equation (25), with the same total vibrational cross section $\sigma_i(v)$ and elastic cross section as those used in the CO-model simulation previously described. The comparison between the transport coefficients from the simulation and from the two-term Boltzmann analysis is shown in Table 5*b*. No significant differences were found, indicating that in this case neither the use of equation (24) nor the two-term approximation leads to significant error.

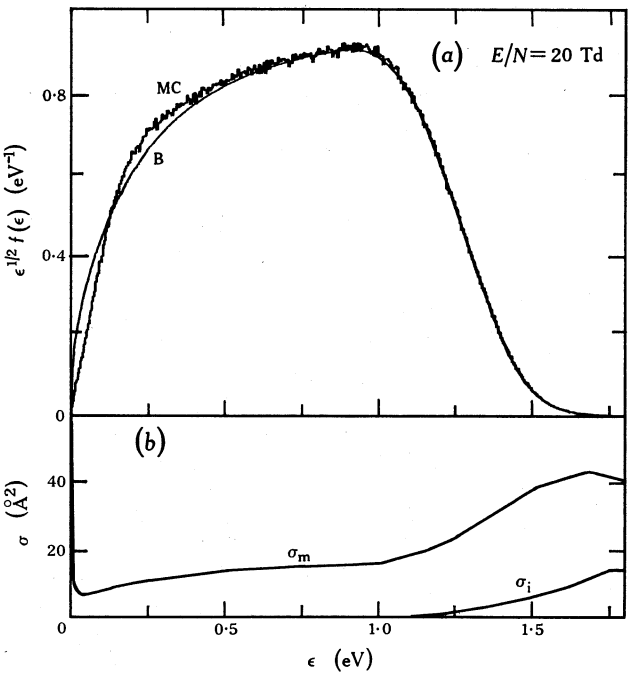

Fig. 4. Electron energy distribution functions (*a*), from the Boltzmann analysis (B) and the Monte Carlo simulation (MC), and cross sections (*b*) for the CO model.

Table 5. Comparison of values of v_{dr}, $\langle\varepsilon\rangle$ and $D_\perp$ for CO model

E/N (Td)	C (10^6)	v_{dr} values (10^6 cm s^{-1}) v_{dr}(B)	v_{dr}(MC)	$\langle\varepsilon\rangle$ values (eV) $\langle\varepsilon\rangle$(B)	$\langle\varepsilon\rangle$(MC)	$D_\perp$ values (10^5 cm^2 s^{-1}) $D_\perp$(B)	$D_\perp$(MC)	$D_\perp$(H)
			(*a*) *Isotropic elastic and inelastic scattering*					
20·0	7·5	2·628	2·595	0·717	0·718	1·044	1·054	1·046
			(*b*) *Isotropic elastic scattering, anisotropic inelastic scattering*					
20·0	7·5	2·628	2·645	0·717	0·721	1·044	1·050	1·047

(ii) *Anisotropic Total Scattering*

The work described in this paper was initiated as part of an overall program to resolve the discrepancies between the vibrational excitation cross sections for hydrogen near threshold, as determined by beam and swarm experiments. One possible explanation is inadequacy of the transport theory used to analyse the swarm results.

In the E/N range (10–25 Td) where the transport coefficients show a maximum sensitivity to the first vibrational cross section near threshold (Crompton *et al.* 1970), more than 50% of the power input to the swarm is dissipated in vibrational excitation (Crompton *et al.* 1969). Moreover, in the energy range of interest, the sum of the rotational excitation cross sections is never more than about 10% of the total cross section. It is therefore reasonable to simulate electron transport in hydrogen for $E/N \sim 20$ Td using a model with a single inelastic channel. Because of the approximately linear increase of the vibrational excitation cross section near threshold and the slow variation of the elastic cross section in the energy range 0·1–2 eV, a model of the form described in subsection *a*(ii) above can be used.

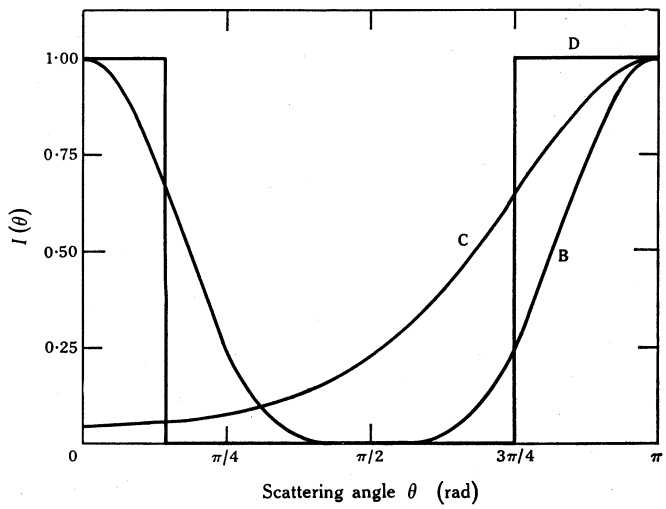

Fig. 5. Angular distributions $I(\theta)$ used for the anisotropic total scattering models: curve B, $I(\theta) = \cos^4\theta$; curve C, $I(\theta) = \exp\{-1{\cdot}5(\cos\theta + 1)\}$; curve D, distribution with strong forward and back scattering (see text).

This model was used to test the effect of anisotropic total scattering, and had the following characteristics:

Molecular weight	$M = 2{\cdot}0$ a.m.u.	
Elastic momentum transfer cross section	$\sigma_{m,e} = 10$ Å^2	
Inelastic threshold	$\varepsilon_i = 0{\cdot}516$ eV	
Inelastic cross section	$\sigma_i(\varepsilon) = 0$	for $\varepsilon < \varepsilon_i$
	$= 0{\cdot}4(\varepsilon - \varepsilon_i)$ Å^2	for $\varepsilon \geqslant \varepsilon_i$
Gas temperature	$T = 0$ K	
Gas number density	$N = 10^{17}$ cm^{-3}	
Drift field	$E = 25{\cdot}0$ V cm^{-1}	

The investigation can be divided into two parts, according to whether the angular scattering distribution $I(\theta)$ is symmetric about $\theta = \frac{1}{2}\pi$ or not.

Symmetric scattering. The two angular distributions chosen were characterized by:

(A) isotropic scattering $I(\theta) = 1$,

(B) pronounced forward and back scattering $I(\theta) = \cos^4\theta$.

The angular distribution B is illustrated in Fig. 5, and the results of the simulation are compared with those from the Boltzmann analysis in Table 6 (cases A and B). There is a significant difference ($\sim 5\%$) only in the values of $D_\perp$ for case B.

Table 6. Comparison of values of v_{dr}, $\langle\varepsilon\rangle$ and $D_\perp$ for hydrogen-like model

Case	E/N (Td)	C (10^6)	v_{dr} values (10^6 cm s^{-1})		$\langle\varepsilon\rangle$ values (eV)		$D_\perp$ values (10^5 cm^2 s^{-1})		
			v_{dr}(B)	v_{dr}(MC)	$\langle\varepsilon\rangle$(B)	$\langle\varepsilon\rangle$(MC)	$D_\perp$(B)	$D_\perp$(MC)	$D_\perp$(H)
A	25·0	20·0	5·27	5·26	1·232	1·234	2·003	1·984	2·000
B	25·0	10·0	5·27	5·24	1·232	1·229	2·003	1·898	1·999
C	25·0	10·0	5·27	5·13	1·232	1·216	2·003	1·919	—
D	25·0	10·0	5·27	5·12	1·232	1·210	2·003	1·795	—

Asymmetric scattering. Two angular distributions were chosen to have the same ratio of $\sigma_{m,e}$ to σ_e. These distributions, also illustrated in Fig. 5, were characterized by:

(C) predominantly back scattering $\quad I(\theta) = \exp\{-1\cdot5(\cos\theta + 1)\}$;

(D) predominantly forward and back scattering

$$I(\theta) = 1 \quad \text{for} \quad 0 < \theta < 0\cdot134\pi,$$
$$= 0 \quad \text{for} \quad 0\cdot134\pi \leqslant \theta < 3\pi/4,$$
$$= 1 \quad \text{for} \quad 3\pi/4 \leqslant \theta.$$

For these distributions $\sigma_{m,e} = 1\cdot438\,\sigma_e$. In order to keep the transport properties approximately the same as those for the symmetric scattering models, the total elastic scattering cross section was reduced to $6\cdot954$ Å^2 thus maintaining $\sigma_{m,e}$ at $10\cdot0$ Å^2. The results of the simulations with these models are shown in Table 6 (cases C and D). There is a significant difference ($\sim 4\%$) between the values of $D_\perp$ obtained from the analysis and from the simulation for case C, and a serious discrepancy ($\sim 12\%$) for case D. In each case there is a difference of the order of 3% in the values of v_{dr} and 2% in $\langle\varepsilon\rangle$. This difference is presumably due to the approximation inherent in the use of equation (4) for $\sigma_m(v)$, since there is no corresponding difference for case B where there is marked anisotropy but $\sigma_{1,i} = 0$. (This conclusion is confirmed by S. L. Lin and colleagues (personal communication) whose calculations for the same model in the two-term approximation did not involve the approximation of equation (4).)

5. Discussion

The five models for which results were given in Section 4 were chosen to illustrate specific points which will be discussed below, but some general conclusions can be drawn from the results obtained for all models.

From Fig. 2 and Table 3 it can be seen that, at a given E/N, there can be significant differences between the energy distribution functions derived from the Boltzmann analysis and from the simulations even when the differences between the transport coefficients are small. This is not unexpected since v_{dr}, $\langle\varepsilon\rangle$ and $D_\perp$ are averages taken over the whole distribution function, but it is fortunate in that it extends the range of validity of the conventional analytical method in situations where the analysis of swarm experiments rests on data for v_{dr} and $D_\perp$ alone. However, circumstances can be envisaged in which errors in the calculated distribution functions at low energies could lead to misinterpretation of experimental data for a

transport coefficient; for example, an attachment coefficient for a gas where the attachment cross section was large at low energies but small at higher energies.

Where there are significant errors in the analytically derived (Boltzmann) transport coefficients, the errors are always much larger in $D_\perp$ than in v_{dr} or $\langle\varepsilon\rangle$. Moreover $D_\perp(\mathrm{H})$, the value of $D_\perp$ calculated using equation (7) and the energy distribution function from the simulation, is always much closer to the analytically derived value than the value derived directly from the simulation using equation (20). Now the formula for $D_\perp$ consistent with the order of approximation used in the conventional Boltzmann analysis is given by equation (7), while the formula for v_{dr} without approximation is

$$v_{dr} = \frac{1}{3}\left(\frac{2}{m}\right)^{\frac{1}{2}} \int_0^\infty \varepsilon f_1(\varepsilon)\, \mathrm{d}\varepsilon . \tag{26}$$

The use of equation (26) with $f_1(\varepsilon)$ derived from the Boltzmann analysis leads to values of v_{dr} that are generally in agreement with those from the simulation. Moreover, the values of $D_\perp$ calculated using equation (7) with $f_0(\varepsilon)$ derived either from the Boltzmann analysis or from the simulation are also, with some exceptions, in good agreement. It appears therefore that the errors in the analytically derived values of $f_0(\varepsilon)$ and $f_1(\varepsilon)$ that result from the approximations do not lead to large errors in the transport coefficients but that, where large errors occur, they can be attributed to the approximate form of equation (7).

Constant Cross Section; Isotropic Scattering

This model was chosen in order to get some feel for how large the ratio of σ_i/σ_e has to be before, in the most favourable circumstance of isotropic total scattering, significant errors result from the use of the conventional analysis. From Tables 1 and 2 it can be seen that v_{dr} and $D_\perp$ are determined with acceptable accuracy up to values of the ratio σ_i/σ_e of 0·5 and 0·1 respectively. The slow variation of the errors with E/N shown by the results for model 2 (see Fig. 3) suggests that, even if $E/N = 24$ Td is not the value at which the maximum errors in v_{dr} and $D_\perp$ occur, the general conclusions are unlikely to be upset.

For comparison it is interesting to note that, if one were to simulate the first (010) vibrational excitation cross section in CO_2 by a cross section that is constant above threshold, then the ratio of σ_i/σ_e would be of the order of 0·1. The cross section decreases for energies above about 0·15 eV, and the energy loss associated with the excitation is only about 0·08 eV rather than the 0·2 eV loss assumed for this model. Even though both these factors would tend to reduce the errors in the transport coefficients calculated from the Boltzmann analysis, the effect of anisotropic scattering could more than compensate for any reduction. Electron transport in CO_2 therefore seems to be a case in which a detailed examination needs to be made of the adequacy of the conventional transport theory.

'Ramp' Inelastic Cross Sections

Extensive simulations were carried out with this model because the smooth variation of the cross sections allowed the Boltzmann code to function satisfactorily and because the energy dependence of the cross sections allowed the 'direct' simulation method to be used. Although the results obtained are specific to a 'gas' with an atomic

weight of 4 and an inelastic energy loss of 0·2 eV, they suggest that the threshold slope of an inelastic cross section has to be comparatively large ($\sim 2{\cdot}0\,\text{Å}^2\,\text{eV}^{-1}$) for a realistic elastic cross section of $6{\cdot}0\,\text{Å}^2$ before the analytical results become seriously in error, provided the scattering is isotropic.

CO Model

The development of the null collision method made it possible to examine a model with arbitrarily varying cross sections and opened the possibility of studying a model more closely approximating a real gas, in this case CO. The model was used in a simulation at a value of E/N where the energy distribution function and transport coefficients are sensitive to the vibrational cross section. The results of the simulation are significant in that they provide a check of the accuracy of the Boltzmann results using realistic scattering parameters, apart from the fact that the elastic scattering was assumed to be isotropic.

The results given in Table 5 suggest that no serious errors are likely to result from the application of the standard Boltzmann analysis to the calculation of $f(\varepsilon)$, v_{dr} and $D_\perp$ in CO for $E/N \leqslant 20$ Td. However, it should be emphasized that these results cannot be regarded as ruling out altogether the possibility of a breakdown of the validity of the analysis as applied to CO or mixtures containing CO given the importance of anisotropy in the total scattering, as demonstrated by the results for the hydrogen-like model. A systematic study of the problem must await the application of computer codes based on more accurate solutions of the Boltzmann equation (e.g. Lin *et al.* 1979) because of the immense amount of computer time required to make such a study using simulation techniques.

Hydrogen-like Model

The comparisons between the analytical results and those from the simulation for a model in which all scattering is anisotropic was carried out only for the hydrogen-like model. In order to exaggerate the consequences of a breakdown of the validity of the conventional analysis as applied to hydrogen in the low energy regime, the threshold slope of the vibrational cross section was made a factor of 2 larger than the slope determined by Crompton *et al.* (1970) from an analysis of swarm data for para-hydrogen. The results in Table 6 show that the consequences of marked anisotropy are likely to be serious. From the results obtained with the first model with a ramp inelastic cross section, it is not surprising to see no significant difference between the two sets of data for v_{dr} and $D_\perp$ when the scattering is isotropic. However, in all three cases where the scattering is anisotropic the analytically determined values of $D_\perp$ are significantly in error even though the error is large only in case D. Significant errors arise in the analytically determined values of v_{dr} and $\langle\varepsilon\rangle$ only when $\sigma_{1,\text{i}} \neq 0$. These conclusions are supported by the recent work of S. L. Lin and colleagues (personal communication), who have developed a numerical solution of Boltzmann's equation, avoiding the approximations described in Section 2, and have applied it to the model discussed here.

6. Conclusions

Although there have been predictions of the general conditions under which the assumptions inherent in the conventional Boltzmann analysis of electron transport

in molecular gases might become invalid, there appears to have been no quantitative work of the type described in this paper. The provision of data for some simple models by means of Monte Carlo simulations has made it possible to demonstrate quantitatively the errors that arise in some specific situations. Although the study is necessarily limited, it has been shown that there are some situations in which the conventional analysis is clearly adequate, and others that require further detailed study to establish when (i.e. over what range of E/N) it can be validly applied. One such investigation has been carried out for molecular hydrogen and is reported in the following paper by Reid and Hunter (1979; present issue pp. 255–9).

The very large number of electron trajectories that must be followed to obtain the required accuracy makes simulation techniques too costly for carrying out extensive surveys, and there is the same problem with their use for the analysis of swarm data where it can be shown that the conventional analytical method is insufficiently accurate. It is to be hoped that more accurate numerical solutions of Boltzmann's equation such as that of Lin *et al.* (1979) will provide the ultimate solution to the problem.

Acknowledgments

The author would like to thank Dr R. W. Crompton for his considerable support and encouragement during the course of this investigation. Assistance was also received from Dr S. R. Hunter and Professor H. R. Skullerud, both of whom provided independent verification of some of the Monte Carlo results; from Dr G. N. Haddad, who carried out additional computing in the author's absence; and from Dr S. L. Lin, Dr R. E. Robson and Dr E. A. Mason, who applied their newly developed analysis program to some of the models and supplied their results in advance of publication. The author is grateful for the cooperation he has received from these colleagues. The receipt of a Commonwealth Postgraduate Research Award during part of this work is acknowledged.

References

Blevin, H. A., Fletcher, J., and Hunter, S. R. (1978). *Aust. J. Phys.* **31**, 299.
Braglia, G. L. (1977). *Physica* B **92**, 91.
Crompton, R. W., Gibson, D. K., and McIntosh, A. I. (1969). *Aust. J. Phys.* **22**, 715.
Crompton, R. W., Gibson, D. K., and Robertson, A. G. (1970). *Phys. Rev.* A **2**, 1386.
Ehrhardt, H., Langhans, L., Linder, F., and Taylor, H. S. (1968). *Phys. Rev.* **173**, 222.
Ferrari, L. (1977). *Physica* C **85**, 161.
Frost, L. S., and Phelps, A. V. (1962). *Phys. Rev.* **127**, 1621.
Gerjuoy, E., and Stein, S. (1955). *Phys. Rev.* **97**, 1671.
Gibson, D. K. (1970). *Aust. J. Phys.* **23**, 683.
Hammersley, J. M., and Handscomb, D. D. (1964). 'Monte Carlo Methods' (Methuen: London).
Holstein, T. R. (1946). *Phys. Rev.* **70**, 367.
Hunter, S. R. (1977). *Aust. J. Phys.* **30**, 83.
Huxley, L. G. H., and Crompton, R. W. (1974). 'The Diffusion and Drift of Electrons in Gases' (Wiley–Interscience: New York).
Land, J. E. (1978). *J. Appl. Phys.* **49**, 5716.
Lin, S. L., and Bardsley, J. N. (1977). *J. Chem. Phys.* **66**, 435.
Lin, S. L., Robson, R. E., and Mason, E. A. (1979). Moment theory of electron drift and diffusion in neutral gases in an electrostatic field. *J. Chem. Phys.* (in press).
McIntosh, A. I. (1974). *Aust. J. Phys.* **27**, 59.
Milloy, H. B., and Watts, R. O. (1977). *Aust. J. Phys.* **30**, 73.

Reid, I. D., and Hunter, S. R. (1979). *Aust. J. Phys.* **32**, 255.
Saelee, H. T., and Lucas, J. (1977). *J. Phys.* D **10**, 343.
Schulz, G. J. (1976). *In* 'Principles of Laser Plasmas' (Ed. G. Bekefi) (Wiley: London).
Skullerud, H. R. (1968). *J. Phys.* D **1**, 1567.
Skullerud, H. R. (1977). Proc. 13th Int. Conf. on Phenomena in Ionized Gases, Berlin, September 12–17 (Physical Society of GDR: Berlin).

Manuscript received 11 January 1979